Nondispersive hole transport in carbazole- and anthracene-containing polyspirobifluorene copolymers studied by the charge-generation layer time-of-flight technique. J Appl Phys 99:...

ARTICLE *in* JOURNAL OF APPLIED PHYSICS · FEBRUARY 2006

Impact Factor: 2.18 · DOI: 10.1063/1.2168590

AIP | Journal of Applied Physics

Nondispersive hole transport in carbazole- and anthracene-containing polyspirobifluorene copolymers studied by the charge-generation layer time-of-flight technique

Frédéric Laquai, Gerhard Wegner, Chan Im, Heinz Bässler, and Susanne Heun

Citation: J. Appl. Phys. **99**, 033710 (2006); doi: 10.1063/1.2168590
View online: http://dx.doi.org/10.1063/1.2168590
View Table of Contents: http://jap.aip.org/resource/1/JAPIAU/v99/i3
Published by the AIP Publishing LLC.

Nondispersive hole transport in carbazole- and anthracene-containing polyspirobifluorene copolymers studied by the charge-generation layer time-of-flight technique

Frédéric Laquai[a] and Gerhard Wegner
Max Planck Institute for Polymer Research Mainz, Ackermannweg 10, D-55128 Mainz, Germany

Chan Im
Department of Chemistry and Research Center for Organic Displays, Konkuk University, 1 Hwayang-dong, Kwangjin-gu, Seoul 143-701, Korea

Heinz Bässler
Institute of Physical, Macromolecular and Nuclear Chemistry and Material Science Center, Philipps University Marburg, Hans-Meerwein-Strasse, D-35032 Marburg, Germany

Susanne Heun
Merck OLED Materials GmbH, Industrial Park Hoechst, D-65926 Frankfurt am Main, Germany

(Received 7 September 2005; accepted 16 December 2005; published online 14 February 2006)

Nondispersive hole transport in two polyspirobifluorene copolymers containing either 10% anthracene or 10% carbazole was studied in detail by the charge-generation layer time-of-flight (TOF) technique over a wide range of electric fields and temperatures. The TOF transients of both polymers showed a clear plateau indicating nondispersive transport of charge carriers. Zero-field mobilities were found to be in the order of 10^{-6} $cm^2/V\,s$ at room temperature. Results were analyzed within the framework of the Gaussian disorder model to extract the parameters of the charge-carrier transport. The width of the transport density of states was determined to be 83 meV for the polyspirobifluorene-anthracene copolymer and 89 meV for the polyspirobifluorene-carbazole copolymer. At lower temperatures a change of slope in the temperature dependence of the zero-field mobility was observed. At higher temperatures the TOF transients were modified by a cusp. Both phenomena can be explained within the framework of the Gaussian disorder model. © *2006 American Institute of Physics*. [DOI: 10.1063/1.2168590]

I. INTRODUCTION

The charge-carrier mobility of π-conjugated polymers is one of their most important parameters that has to be taken into account whenever a polymer is considered for application as an active material in solid-state devices such as organic light-emitting diodes[1,2] (OLEDs) and flexible organic thin-film transistors (OTFTs).[3] In the past, different techniques have been used to determine the charge-carrier mobility. These are, for instance, space-charge-limited steady-state–current-voltage measurements applying Child's law to extract the charge-carrier mobility, dark injection space-charge-limited current (DI SCLC) transient measurements, or the time-of-flight (TOF) method.[4,5] The latter monitors the movement of an initially created charge-carrier package through a bulk and determines the transit time that the charge carriers need to arrive at the counterelectrode. However, each method has its drawbacks. The space-charge-limited steady-state–current-voltage measurements cannot be applied if the charge-carrier mobility is field dependent, as found for almost all organic materials, or if traps are present in the material. Moreover, it renders an average value for the mobility since it has to be extracted from the current density as a function of the applied voltage. The DI SCLC method measures the current transient and delivers a transit time for the charge carriers, but it requires Ohmic injection from the contacts and trap-free materials to observe the characteristic temporal evolution with a maximum in the current transient. The TOF method, which has been widely used to study charge-carrier mobilities in molecularly doped crystals and polymers,[6] requires relatively thick films in the micron range often prepared by drop casting from a polymer solution. Since film morphology is of crucial importance for charge-carrier mobility, drop-casted films are not always comparable to spin-coated ones. Therefore, TOF measurements using drop-casted thick films can lead to different results to those obtained with spin-casted thin films,[7] as commonly used in organic/polymeric devices. Furthermore, if charge carriers are created intrinsically by illuminating the polymer under investigation directly, even thicker polymer films have to be used to keep the spatial extension of the charge-carrier package sufficiently small in comparison to the film thickness. This problem can be circumvented by using a separate charge-carrier generation layer which consists, for example, of a small molecular dye.[8] Recently, Markham *et al.* reported the application of a perylene-diimide derivative as a thin charge-carrier generation layer (CGL) in TOF measurements.[9] Using this method, they were able to measure the mobility even in thin spin-coated films. Very recently, we reported nondispersive hole transport in tetraalkoxy-

[a]Author to whom correspondence should be addressed; electronic mail: laquai@mpip-mainz.mpg.de

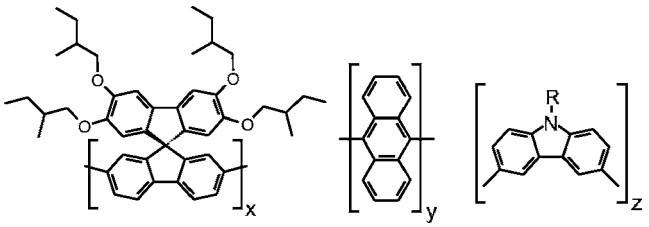

FIG. 1. Chemical structure of the investigated polyspirobifluorene copolymers. The compositions of polymer 1 (polyspirobifluorene anthracene) are $x=0.9$ and $y=0.1$ whereas it for polymer 2 (polyspirobifluorene carbazole) $x=0.9$ and $z=0.1$.

substituted polyspirobifluorene-type polymers studied by the charge-generation layer TOF method.[10] Apart from the polyfluorenes, the polyspirobifluorene polymers are very promising candidates for blue light-emitting diodes due to their higher thermal and oxidative stabilities, excellent solubility, and film-forming properties. The spiroconcept was originally derived from small molecular compounds by Salbeck *et al.* to stabilize the amorphous glassy state of fluorophores by adjusting their glass transition temperature.[11,12] Meanwhile, small molecular spirocompounds have proven their applicability in organic LEDs,[13,14] solid-state dye-sensitized solar cells,[15] and organic lasers.[16–18] Spirocopolymers that can be cross-linked in solid state have proven their potential in patterned multicolor organic light-emitting displays.[19] The charge-carrier mobilities of small molecular spiromaterials were studied by Bach *et al.* for 2,2',7,7'-tetrakis(*N,N*-diphenylamine)-9,9'-spirobifluorene (spiro-TAD) and 2,2', 7, 7'-tetrakis (*N,N*-di-*m*-methylphenylamine)-9, 9'-spirobifluorine (spiro-m-TTB) (Ref. 20) and Poplavskyy *et al.* reported nondispersive hole transport for 2,2',7,7'-tetrakis-(*N,N*-di-4-methoxyphenylamino)-9,9'-spirobifluorine (spiro-MeOTAD).[5]

In the present study we were interested in the charge-carrier transport properties of two polyspirobifluorene copolymers which contain either 10% anthracene or 10% carbazole in comparison to our previously reported results on a spirohomopolymer and a triarylamine-containing polyspirobifluorene copolymer (Fig. 1). The results of the field- and temperature-dependent mobility measurements were interpreted in the framework of the Gaussian disorder model proposed by Borsenberger *et al.*[21] in order to extract the charge transport parameters of both materials. These are, for example, the energetic disorder parameter σ and the positional disorder parameter Σ. The mobility measurements were performed over a wide range of temperatures to check for the thermal stability of the polymers and to study the transition from a nondispersive to a dispersive transport regime at lower temperature. We will show that the disorder model describes the hole transport even in the dispersive transport regime and we will discuss the occurrence of a cusp that can be observed in the TOF transients at elevated temperatures.

II. EXPERIMENT

The polyspirobifluorene copolymers investigated in this study were synthesized by Merck OLED Materials GmbH. Their synthesis has been described elsewhere.[22,23] Both materials have high solubility in common organic solvents, excellent film-forming properties, and high thermal as well as oxidative stabilities. Their molecular weight MN was determined to be 1.2×10^5 g/mol for polymer 1 and 1.1×10^5 g/mol for polymer 2 versus polystyrene standard in toluene. They can be used as active materials in blue polymer light-emitting diodes (PLEDs), polymer 1 rendering 2.6 cd/A at Commission Internationale de l'Eclairage (CIE) coordinates of (0.16/0.17), and polymer 2 with 2.0 cd/A at (0.16/0.12).[24] The alkyl-substituted perylene-diimide (PDI) derivative (2,9-di(pent-3-yl)-anthra[2,1,9-def:6,5,10-d′e′f′] diisoquinoline-1,3,8,10-tetrone) was chosen as charge-generation material. Its highest occupied molecular-orbitial (HOMO) energy is almost equal or slightly below the energy of the HOMO of the polyspirobifluorene copolymers. Hence, the condition for sensitized charge-carrier injection is fulfilled in our test system. The dye was used as delivered from Sensient Imaging Technologies GmbH. Films for TOF measurements were spin coated at 700 rpm onto carefully cleaned indium tin oxide (ITO) substrates from toluene solutions, using concentrations of 2 wt % for polymer 1 and 5 wt % for polymer 2. Film thicknesses were measured with a TENCOR P-10 surface profiler and determined to be 1.6 μm for polymer 1 and 1.6 μm for polymer 2. The films were kept in high vacuum overnight to remove residual solvent. A thin film ($\sim$10 nm) of the substituted PDI derivative was then deposited onto the polymer film through a shadow mask at pressures of 10^{-6} mbar. Subsequently, aluminum counterelectrodes with a diameter of 4 mm and a thickness of approximately 100 nm were evaporated without breaking the vacuum. For TOF measurements, the sample was housed in a temperature-controlled home-built cryostat under a dynamic vacuum of typically 10^{-5} mbar. Excitation at 537 nm was provided by an optical parametric oscillator (OPO) (GWU Lasertechnik GmbH, Germany) pumped by the third harmonic of a Nd:YAG (yttrium aluminum garnet) laser. Typical excitation intensities were in the range from 1 to 2 μJ/pulse. The samples were illuminated from the ITO side and the current transient was detected with a Tektronix oscilloscope (TDS 524A) triggered by the laser pulse. The excitation intensity was chosen to generate not more than 5% of the charge stored at the device interface to avoid space-charge effects and the *RC* time constant of the circuit was kept sufficiently small in order not to distort the TOF transients.

III. RESULTS AND DISCUSSION

The device configuration and circuit setup that have been used in this study to measure the charge-carrier transients were described previously.[10] Briefly, the device consists of a relatively thick spin-coated polymer film ($d>1$ μm) and a thin evaporated charge-generation layer ($\sim$10 nm) that consists of a PDI dye, both sandwiched between an ITO and an aluminum electrode. Upon illumination of the PDI at 537 nm (2.31 eV) with short laser pulses (8 ns), excited states are created within the layer of the dye which are successively separated into free charges when an electric field is applied across the device. While electrons are removed from the

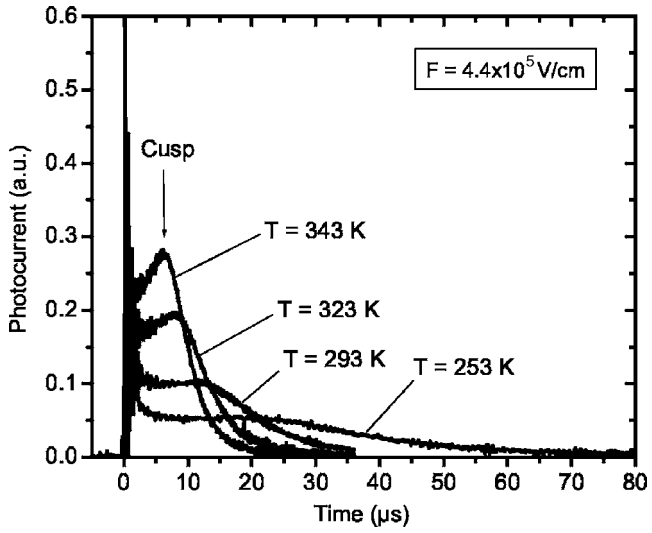

FIG. 2. Representative TOF transients for polymer 1 (polyspirobifluorene anthracene) at $T=343$ K, $T=323$ K, $T=293$ K, and $T=253$ K at constant electric field. A cusp develops at higher temperatures. At lower temperatures, the tail of the transient signal lengthens, a signature of dispersive transport.

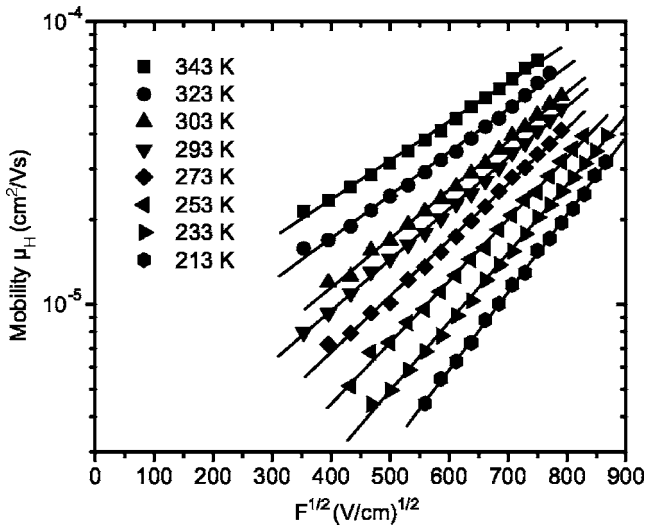

FIG. 3. Hole mobility of polymer 1 as a function of $F^{1/2}$ in semilogarithmic representation at a selection of temperatures. The lines are fits to the experimental data.

CGL into the positively biased aluminum electrode, holes are injected into the polymer film and transported through the device. Since the CGL is very thin in comparison to the polymer film and almost no injection barrier should exist at the interface to the polymer, charge transport in the CGL can be neglected and the measured TOF transients represent the charge transport features of the investigated polymer.

Figure 2 shows representative TOF transients of the polyspirobifluorene-anthracene copolymer (polymer 1) at different temperatures at constant electric field. The room-temperature ($T=293$ K) TOF transient shows a clear plateau indicative of nondispersive transport with a pronounced tail that represents the diffusion broadening of the charge-carrier package during its transport through the polymer film. At higher temperatures, the TOF transients are modified by the emergence of a cusp. The cusp becomes more pronounced with increasing temperature. The origin of this cusp is important for charge-carrier transport within a disordered density of transport states, as will be discussed later. At lower temperatures, the length of the tail of the TOF transients increases but the plateau persists even at the lowest temperatures investigated in this study. The transit time of the charge-carrier package can be determined from the intersection of asymptotes to the plateau and the tail. This corresponds to the time when the charge-carrier package starts arriving at the counterelectrode. Using this method one has to take into consideration that one keeps mainly track of the fastest charge carriers. Recent studies of charge-carrier transport in conjugated materials have shown that a transit time which corresponds to the time at which the amplitude of the transient has decayed to half or even to a quarter of its initial value leads to results which are better comparable to those obtained from SCLC measurements.[25,26] However, the functional dependencies are independent of data analysis, though the absolute values may change to lower mobility. For a better comparison with our recent results of mobility measurements on polyspirobifluorene polymers and former results on conjugated polymers, we chose the first method to determine the transit time and calculated the charge-carrier mobility using the equation

$$\mu = \frac{d}{t_{\mathrm{tr}} F}. \tag{1}$$

Here, d represents the sample thickness in centimeters, F the electric field, and t_{tr} the transit time obtained from the TOF signals. The TOF measurements were performed over a wide range of electric fields and temperatures. Figure 3 depicts the hole mobility of polymer 1 as a function of the electric field at different temperatures. The mobilities follow a $\ln \mu \propto F^{1/2}$ dependence on the electric field at all temperatures investigated. Further, the slope β of the field dependence increases with decreasing temperature. Such behavior has been described by Borsenberger *et al.*[21] and Bässler[27] in their disorder formalism of charge-carrier transport. The disorder formalism assumes an energetic and a positional distribution of transport sites which are both of Gaussian shape. The former is called diagonal disorder and described by the disorder parameter σ which corresponds to the width of the transport density of states, whereas the latter is called off-diagonal disorder described by the positional disorder parameter Σ. The model takes into account neither the history of the charge carrier during its migration through the density of states nor any correlation between different transport sites. Moreover, the transport sites are considered as points having no spatial extension which is a somewhat questionable simplification of the reality in conjugated polymers. Within these limitations, Monte Carlo simulations performed on such a system of disordered transport sites predicted for the mobility μ a dependence on the electric field F and temperature T, as expressed in the equation

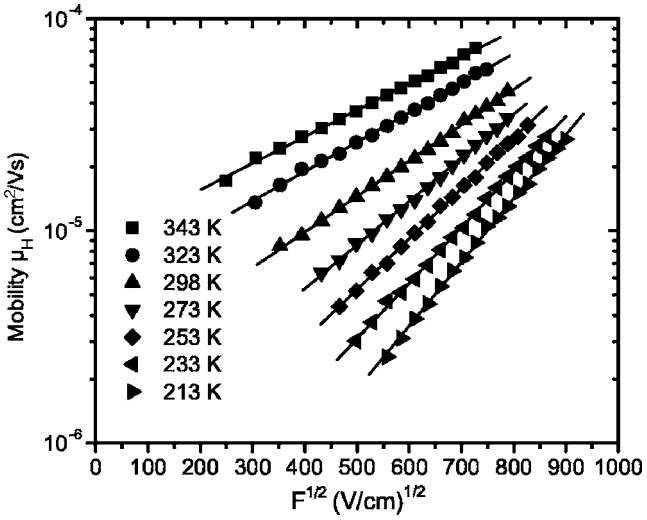

FIG. 4. The field dependence of hole mobility of polymer 2 for a selection of temperatures in a semilogarithmic plot.

$$\mu = \mu_0 \exp\left[-\left(\frac{2\sigma}{3kT}\right)^2\right] \exp C_0\left[\left(\frac{\sigma}{kT}\right)^2 - \Sigma^2\right]\sqrt{F}, \qquad (2)$$

where μ_0 is the mobility prefactor, σ and Σ are the energetic and positional disorder parameters, and C_0 is a constant which reflects the hopping distance that a charge carrier has to overcome to be transferred from one site to another. For the system in the simulations, a C_0 of $2.9\times10^{-4}(\mathrm{cm/V})^{1/2}$ was obtained for an intersite hopping distance of 0.6 nm.

Equation (2) predicts a linear dependence of $\ln \mu \propto F^{1/2}$ for the mobility on the electric field, as observed for both polymers investigated in this study (see Figs. 3 and 4). Extrapolation to $F=0$ renders the so-called zero-field mobility. As also predicted from Eq. (2), plotting $\log \mu(F=0,T)$ as a function of $1/T^2$ leads to a linear dependence (see Figs. 5 and 6) from which the energetic disorder parameter σ and the mobility prefactor μ_0 are obtained. Further, plotting the slopes β of the field dependencies against $(\sigma/kT)^2$ (not shown here) gives access to the positional disorder parameter

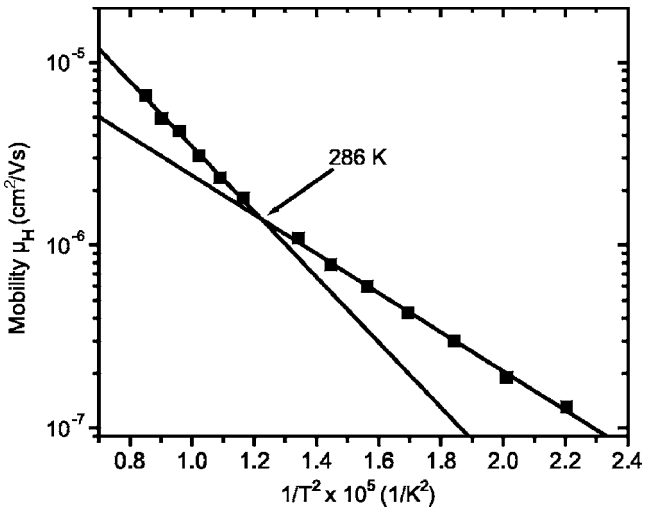

FIG. 5. The zero-field hole mobility μ_H $(F=0,T)$ plotted vs $1/T^2$ in a semilogarithmic fashion. Notice the change of slope as the transport becomes dispersive.

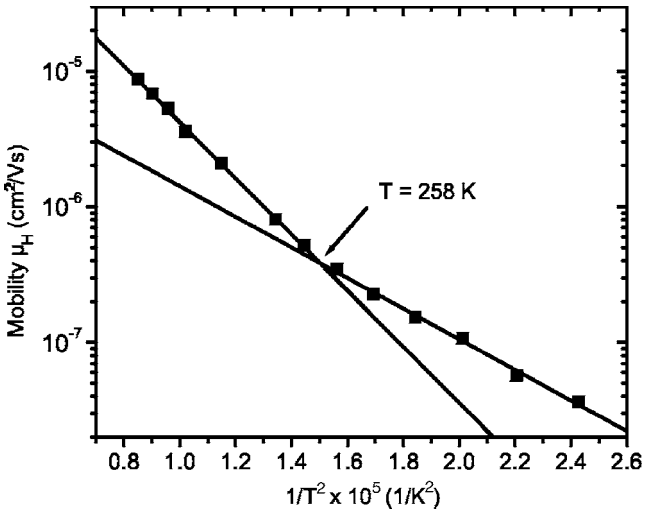

FIG. 6. The extrapolated zero-field mobilities as a function of $1/T^2$ for polymer 2. The lines are linear fits to the data. Notice the transition to the dispersive transport regime below $T=258$ K indicated by the change of slope.

Σ and the intersite hopping constant C_0. However, due to the above-mentioned limitations, especially the point shape of the molecules that was used to derive Eq. (2), these values may have some intrinsic uncertainty and should be interpreted carefully. Nevertheless, it should be possible to compare structurally similar compounds among each other.

The charge transport parameters derived from fitting the experimentally obtained mobility data are summarized in Table I. Both polymers exhibit a zero-field mobility which is in the order of 10^{-6} cm^2/V s at room temperature. For electric fields above 5×10^5 V/cm, very common for conventional organic LEDs, the mobility reaches values in the order of 10^{-5} cm^2/V s. These values are comparable to the charge-carrier mobility found for a spirohomopolymer. Recently, we reported the results from TOF experiments on that polymer[10] and compared the obtained mobility values and charge transport parameters with those of other conjugated polymers, for instance, the far more ordered methyl-substituted ladder-type poly-p-phenylene (MeLPPP),[28,29] an alkylsubstituted polyfluorene (PFO),[30,31] and poly(2–methoxy-5–(2'-ethylhexyloxy)-1,4–phenylene-vinylene) (MEH-PPV).[32] Not only are the charge transport mobilities observed for both polymers in this study similar to the previously reported homopolymer but also the width of the transport density of states and the intersite hopping constant C_0 are of similar values. Thus, the incorporation of anthracene or carbazole does not significantly change the transport properties which can be understood since the HOMO energy of carbazole and anthracene is below the HOMO energy of the alkoxy-substituted spirobifluorene ($\sim$−5.3 eV) backbone.[10] The data thus reflect an in-chain dilution with 10% antitraps in both cases. Therefore, we refer for a comparative discussion of the parameters to our previous report.[10] In the study presented herein, we will concentrate more deeply on the features of sensitized charge-carrier generation, the observation of a cusp at higher temperatures, and the occurrence of a change of slope in the temperature dependence of the zero-field mobility at lower temperatures.

TABLE I. Charge-carrier transport parameters of polymers 1 and 2.

Material	μ_H ($cm^2/V\,s$)	μ_0 ($cm^2/V\,s$)	σ (eV)	C_0 $(cm/V)^{1/2}$	Σ
Spiro anthracene (1)	1.8×10^{-6}[a]	2.1×10^{-4}	0.083[b] 0.086[c]	3.4×10^{-4}	≈0
Spiro carbazole (2)	2.1×10^{-6}[a]	4.9×10^{-4}	0.089[b] 0.088[c]	3.6×10^{-4}	1.1

[a]Zero-field mobility at room temperature.
[b]Extracted for $T>T_c$ according to Eq. (3a).
[c]Extracted for $T<T_c$ according to Eq. (3b).

Before beginning a discussion of the experimental results, let us briefly recall the scenario of charge-carrier transport in a disordered density of states and charge-carrier generation using bulk excitation or sensitized injection. In the case of bulk generation, the charge carriers are randomly distributed within the density of states after excitation of the polymer. In the case of sensitized injection with a perylene-diimide charge-generation layer, the charge-generation process seems to be by extrinsic charge generation, i.e., Coulombically bound electron-hole pairs form at the interface between the polymer and the dye.[33] Under the applied electric field, these bound pairs dissociate and inject a sheet of holes into the HOMO of the polymer. Since the layer of the dye is very thin and carriers are created at the interface, and since the dye has a distinct HOMO energy, the injected charge-carrier package is not only narrower in its spatial, but also in its energetic distribution compared to bulk charge-carrier generation. In both cases of charge-carrier generation, the injected charge carriers then undergo a fast relaxation process within the density of states to attain their equilibrium energy which depends on the temperature of the system. Under the applied electric field the charge carriers start to move and are successively transported at their equilibrium transport energy within the density of states (DOS) until they reach the counterelectrode. During transport, any upward jump in energy to a neighboring transport site requires an activation energy that can be provided by the electric field or by thermal activation. If deep traps are absent, all carriers are transported with almost the same speed, resulting in a constant current as observed in the TOF transients. However, the initially created charge-carrier package undergoes a diffusive broadening during its migration through the bulk which results in a pronounced tail of the TOF transients. For decreasing temperature, the simulation predicted a change of the slope of the zero-field mobility dependence on temperature as expressed by the following equations:

$$\mu \approx \exp\left[-\left(\frac{2\sigma}{3kT}\right)^2\right], \quad T > T_c, \tag{3a}$$

$$\mu \approx \exp\left[-\left(\frac{\sigma}{2kT}\right)^2\right], \quad T < T_c, \tag{3b}$$

where T_c is expressed by

$$\left(\frac{\sigma}{kT_c}\right)^2 = 44.8 + 6.7 \log d, \tag{4}$$

with d being the film thickness in dimensionless centimeters.[34,35] For temperatures below T_c, the charge carriers cannot attain their dynamic equilibrium any more since the relaxation process towards the dynamic equilibrium is slower, upward jumps and "detours" being impeded by a lack of thermal activation energy. The dependence of the zero-field mobility on temperature decreases as a consequence of an incomplete relaxation process.

This has been qualitatively confirmed in several prior studies of charge transport in conjugated polymers. For our test system, we found that the temperature dependence of the zero-field mobility changes its slope at approximately 286 K for polymer 1 and 258 K for polymer 2 (see Figs. 5 and 6) although the plateau in the transients, indicative of nondispersive transport, remains even below T_c (see Fig. 2). It is remarkable that extracting the width of the transport density of states from the temperature dependence below T_c according to Eq. (3b) leads to very similar values of σ (see Table I), as obtained from the temperature dependence above T_c using Eq. (3a). It thus appears that the disorder formalism does not only give a qualitative description of the change of slope in the $1/T^2$ dependence for conjugated polymers but also a quantitative one. This is a somewhat unexpected result given the aforementioned initial assumptions that were used to derive Eqs. (2) and (3). However, the disorder model also has its limitations since the positional disorder parameter Σ was not taken into account in deriving Eq. (4). This negligence is obviously problematic in the case of an amorphous film of a disordered conjugated polymer that was prepared by spin coating. Hence, the transition temperatures T_c calculated from the σ values are not in accordance with the experimentally observed transition temperatures, and a meaningful positional disorder parameter Σ could not be derived in all cases.

Finally, the emergence of a cusp in the TOF transients at higher temperatures has to be discussed. The observation of a cusp has sometimes been reported in the literature.[36,37] With increasing temperature, the slope of the cusp increased, but the occurrence of the cusp was found to be independent of the applied electric field and laser excitation intensity. The cusp might be an important intrinsic feature of the transport between randomly disordered transport sites rather than caused by space-charge effects as one could suggest. Borsenberger *et al.* suggested an explanation based on the idea that the initial occupancy of charge carriers created in a DOS of

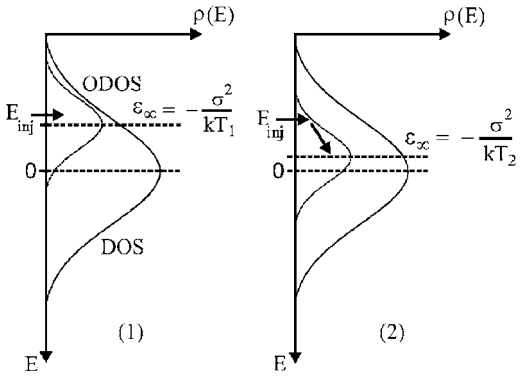

FIG. 7. Representation of the energetic situation of the DOS at room temperature T_1 (1) and at a higher temperature T_2 (2) assuming a constant energy of injection E_{inj}. In case (1) the holes are injected close to their equilibrium energy ε_∞. Transport of charges can occur immediately. In case (2) the holes are injected into the tail of the occupied density of states (ODOS); therefore, they have to reach the transport sites closer to the center of the ODOS before transport can occur. This process may cause the cusp that can be observed at higher temperatures.

localized states is important for the occurrence of a cusp.[38] If charge carriers are generated randomly in the DOS they will relax to their thermal equilibrium energy $\varepsilon_\infty = -(\sigma^2/kT)$ with respect to the center of the DOS and occupy transport sites distributed around the equilibrium energy in a Gaussian shape. This distribution of occupied transport sites is therefore referred to as occupied density of states (ODOS). The relaxation of charge carriers causes a displacement current in the sample that will decay in time. The current settles to a plateau if the relaxation time is shorter than the transit time, otherwise the signal will be dispersive. In the case of sensitized charge-carrier injection the charges can be injected at their quasiequilibrium energy into the DOS. The current will immediately settle to a plateau until the charge carriers arrive at the counterelectrode. On the other hand if the energy at which the charge carriers are injected into the DOS is below there equilibrium energy they have to be heated up to transport sites which are higher in energy in order to be transported within the DOS.

The present results support this idea. The ODOS shifts with increasing temperature closer to the center of the DOS. Thus, at higher temperatures the charge carriers are injected from the CGL into transport sites which are in the tail of the ODOS [situation (2) in Fig. 7]. Hence, in the beginning the charge carriers are trapped in the tail of the ODOS and have to climb up to transport sites which are closer to the equilibrium energy of the ODOS in order to be transported. As a result the speed of the charge carriers increases with time since the density of transport sites increases and more transport sites can be reached by the charge carriers. This may lead to a continuously increasing current as observed in the TOF transients and to the emergence of a cusp that becomes more pronounced at higher temperatures.

IV. CONCLUSIONS

Nondispersive hole transport was observed for an anthracene and a carbazole containing polyspirobifluorene copolymer and studied by the charge-carrier generation layer time-of-flight method. Both polymers exhibit zero-field mobilities which are in the order of 10^{-6} cm^2/V s at room temperature. The mobilities and charge transport parameters were similar to those reported recently for a spirohomopolymer. In conclusion, neither anthracene nor carbazole changes the hole transport properties of alkoxy-substituted spirocopolymers significantly since both comonomers do not act as traps for the charge carriers. This allows the tuning of the optical properties without changing the charge transport features. Of course anthracene and carbazole units can interact with neighboring spirounits and can effectively build concerted transport sites with a concentration of more than 50% if one takes into account an effective conjugation length of at least five repetition units, but this kind of interaction does not seem to influence the transport properties significantly. The field and temperature dependencies of the mobility can be interpreted within the framework of the disorder formalism. Furthermore, even in the transport regime below T_c the predicted $1/T^2$ dependence is obeyed and the change of slope agrees very well with the formalism. The clearly nondispersive room-temperature TOF transients testify on the absence of intrinsic traps and on the high chemical purity of the investigated polymers. Additionally, the $\ln \mu \propto F^{1/2}$ field dependence is obeyed even at temperatures as high as 343 K and beyond, which testifies on the good thermal stability and hole transport stability of polyspirobifluorene polymers. This makes them very promising materials for polymer LED applications.

ACKNOWLEDGMENTS

Financial support by the BMBF (Project No. PT-IT/BD 252) is gratefully acknowledged. One of the authors (F.L.) thanks the Fonds der Chemischen Industrie for providing a Kekulé scholarship. The authors also thank A. Falcou and E. Breuning from Merck OLED Materials GmbH for the polymer synthesis, A. Buesing from the same company, and Dirk Hertel from the University of Cologne for useful discussions. Finally, the authors acknowledge technical assistance by A. Becker and D. Richter.

[1] R. H. Friend *et al.*, Nature (London) **397**, 121 (1999).
[2] J. Steiger, S. Heun, and N. Tallant, J. Imaging Sci. Technol. **47**, 473 (2003).
[3] G. Horowitz, J. Mater. Res. **19**, 1946 (2004).
[4] J. Veres, H. Becker, H. Spreitzer, H. Vestweber, W. Kreuder, *NIP16 Conference Proceedings* (Society for Imaging Science and Technology, Vancouver, BC, Canada, 2000), Vol. 16, p. 335.
[5] D. Poplavskyy and J. Nelson, J. Appl. Phys. **93**, 341 (2003).
[6] P. M. Borsenberger and D. S. Weiss, *Organic Photoreceptors for Xerography* (Marcel Dekker, New York, 1998).
[7] P. M. Borsenberger, L. Pautmeier, and H. Bässler, Phys. Rev. B **46**, 12145 (1992).
[8] C. Im, H. Bässler, H. Rost, and H. H. Hörhold, J. Chem. Phys. **113**, 3802 (2000).
[9] J. P. J. Markham, T. D. Anthopoulos, I. D. W. Samuel, G. J. Richards, P. L. Burn, C. Im, and H. Bässler, Appl. Phys. Lett. **81**, 3266 (2002).
[10] F. Laquai, G. Wegner, C. Im, H. Bässler, A. Büsing, A. Falcou, and S. Heun, J. Appl. Phys. **99**, 023712 (2006).
[11] J. Salbeck, F. Weissörtel, and J. Bauer, Macromol. Symp. **125**, 121 (1997).
[12] J. Salbeck, N. Yu, J. Bauer, F. Weissörtel, and H. Bestgen, Synth. Met. **91**, 209 (1997).
[13] F. Steuber, J. Staudigel, M. Stossel, J. Simmerer, A. Winnacker, H. Spre-

itzer, F. Weissörtel, and J. Salbeck, Adv. Mater. (Weinheim, Ger.) **12**, 130 (2000).
[14]H. Vestweber *et al.*, *Proceedings of Displays and Vacuum Electronics* (ITG-Fachbericht, Garmisch-Partenkirchen, 2001), p. 31.
[15]J. Krüger, R. Plass, M. Grätzel, and H.-J. Matthieu, Appl. Phys. Lett. **81**, 367 (2002).
[16]D. Schneider *et al.*, Adv. Mater. (Weinheim, Ger.) **17**, 31 (2005).
[17]D. Schneider *et al.*, Appl. Phys. Lett. **85**, 1659 (2004).
[18]D. Schneider *et al.*, Appl. Phys. Lett. **84**, 4693 (2004).
[19]C. D. Müller *et al.*, Nature (London) **421**, 829 (2003).
[20]U. Bach, K. De Cloedt, H. Spreitzer, and M. Grätzel, Adv. Mater. (Weinheim, Ger.) **12**, 1060 (2000).
[21]P. M. Borsenberger, L. Pautmeier, and H. Bässler, J. Chem. Phys. **94**, 5447 (1991).
[22]H. Becker, K. Treacher, H. Spreitzer, A. Falcou, P. Stössel, A. Büsing, and A. Parham, World Patent No. PCT WO 03/020790 A2 (2003).
[23]H. Becker, S. Heun, K. Treacher, A. Büsing, and A. Falcou, SID Int. Symp. Digest Tech. Papers **33**, 780 (2002).
[24]S. Heun (unpublished).
[25]A. J. Campbell, D. D. C. Bradley, H. Antoniadis, M. Inbasekaran, W. W. Wu, and E. P. Woo, Appl. Phys. Lett. **76**, 1734 (2000).
[26]D. Poplavskyy, J. Nelson, and D. D. C. Bradley, Macromol. Symp. **212**, 415 (2004).
[27]H. Bässler, Phys. Status Solidi B **175**, 15 (1993).
[28]D. Hertel, U. Scherf, and H. Bässler, Adv. Mater. (Weinheim, Ger.) **10**, 1119 (1998).
[29]D. Hertel, H. Bässler, U. Scherf, and H. H. Hörhold, J. Chem. Phys. **110**, 9214 (1999).
[30]D. Poplavskyy, T. Kreouzis, A. J. Campbell, J. Nelson, and D. D. C. Bradley, Mater. Res. Soc. Symp. Proc. **725**, P.1.4.1 (2002).
[31]M. Redecker, D. D. C. Bradley, M. Inbasekaran, and E. P. Woo, Appl. Phys. Lett. **73**, 1565 (1998).
[32]A. R. Inigo, C. Haan, W. Fann, Y.-S. Huang, G.-Y. Perng, and S.-An Chen, Adv. Mater. (Weinheim, Ger.) **13**, 504 (2001).
[33]Z. D. Popovic, A.-M. Hor, and R. O. Loutfy, Chem. Phys. **127**, 451 (1988).
[34]H. Bässler and P. M. Borsenberger, Chem. Phys. **177**, 763 (1993).
[35]S. Heun and P. M. Borsenberger, Chem. Phys. **200**, 245 (1995).
[36]M. Novo, M. van der Auweraer, F. C. Schryver, P. M. Borsenberger, and H. Bässler, Phys. Status Solidi B **177**, 223 (1993).
[37]A. Ochse, A. Kettner, J. Kopitzke, J.-H. Wendorff, and H. Bässler, Phys. Chem. Chem. Phys. **1**, 1757 (1999).
[38]P. M. Borsenberger, L. Pautmeier, and H. Bässler, J. Chem. Phys. **95**, 1258 (1991).